

**Extraction and Scrub of  
Irradiated MOX Fuel**  
( Document Prepared by Other Institute,  
Based on the Contract )

**February, 2002**

**SUMMIT AEA CORPORATION**

本資料の全部または一部を複写・転載する場合は、下記にお問い合わせください。

〒319-1184 茨城県那珂郡東海村大字村松 4 番地 49

核燃料サイクル開発機構  
技術展開部 技術協力課

Inquiries about copyright and reproduction should be addressed to :

Technical Cooperation Section,  
Technology Management Division,  
Japan Nuclear Cycle Development Institute  
4-49 Muramatsu, Naka-gun, Ibaraki 319-1184  
Japan

© 核燃料サイクル開発機構  
( Japan Nuclear Cycle Development Institute )  
2002

実溶解液を用いた向流抽出試験  
(核燃料サイクル開発機構 契約業務報告書)

Richard Pateman, Roger Paige, Jon Jenkins (\*)

要 旨

本報告書では、小型遠心抽出器を使用した抽出・洗浄試験の結果について以下のとおり報告する。試験は、約10%のプルトニウム含む照射済み MOX 燃料を使用し、室温で行われた。放射性が高いことから、試験はホット・セルの中で行われた。

試験の結論は以下の通り。

1. ウラン、プルトニウムともに、抽出プロセスで回収された率は、99.99%以上と、非常に高かった。抽出器の性能は、有機物中のウラン濃度に関らず安定していた。(標準誤差は、試験中に採取する6サンプルの平均濃度 $\pm$ 3%であった。)
2. 抽出の除染係数は $^{154}\text{Eu}$ と $^{155}\text{Eu}$ でおよそ80から90の間であった。また、 $^{241}\text{Am}$ と $^{244}\text{Cm}$ は、およそ140と170の間で、 $^{134}\text{Cs}$ と $^{137}\text{Cs}$ は、1000以上であった。
3.  $^{154}\text{Eu}$ ,  $^{155}\text{Eu}$ ,  $^{241}\text{Am}$ ,  $^{244}\text{Cm}$ の抽出有機相中の濃度は、MOXのフィードのステージで減少した。恐らくこれは、抽出されたウランとプルトニウムに取って代わられたためであろう。
4. 水相側のMOXフィードのエントレインメントにより、 $^{134}\text{Cs}$ と $^{137}\text{Cs}$ が有機相へ混入したと仮定した場合、これら核種の除染係数から、水相の混入は $<0.1$  ボリューム%以下であることがわかる。この仮定は、収集されたサンプルの目視検査でも立証される。即ち、混入は観察されなかったのである。
5. 洗浄工程において、ウラン・フィードの約7% プルトニウム・フィードの約8%が水相に移行した。
6. 洗浄工程の見かけの除染係数は、 $^{244}\text{Cm}$ で600以上、 $^{134/137}\text{Cs}$ では15、 $^{154/155}\text{Eu}$ では47、 $^{241}\text{Am}$ では約4であった。
7. FPの濃度は、第1洗浄段から第4洗浄段まで、大きな減少はなかった。エントレインメントは、水相の中間ステージにおける2つのサンプルで観察されただけであるが、ステージ間の混入性が高いせいであると思われる。
8. 上記について、その他の可能性としては、有機相へのMOX溶液の飛沫同伴割合が高く、これをほとんどの洗浄段で効果的に取り除くことができなかつたためであると考えられる。

---

本報告書は、サミット AEA 株式会社核燃料サイクル開発機構との契約により実施した業務成果に関するものである。

機構担当課室：環境保全・研究開発センター 先進リサイクル研究開発部 先進再処理技術開発グループ  
\*AEA Technology (英国)

**Extraction and Scrub of Irradiated MOX Fuel**  
(Document Prepared by Other Institute, Based on the Contract)  
Richard Pateman, Roger Paige, Jon Jenkins (\*)

**Abstract**

This report gives the results of extraction and scrub tests with miniature centrifugal contactors. The tests were performed at ambient temperature on irradiated MOX fuel containing approximately 10% Pu. Due to the highly radioactive nature of this material the experiments were performed in a hot-cell.

The conclusions of the tests were as follows.

1. A high recovery (>99.99%) of both U and Pu were achieved by the extraction process. The performance of the contactors was very stable, as demonstrated by the variation of the U concentration in the organic product (standard deviation was  $\pm 3\%$  of the mean concentration for six samples taken during the test).
2. The DFs given by extraction were approximately between about 80 and 90 for  $^{154}\text{Eu}$  and  $^{155}\text{Eu}$ , between 140 and 170 for  $^{241}\text{Am}$  and  $^{244}\text{Cm}$ , and >1000 for  $^{134}\text{Cs}$  and  $^{137}\text{Cs}$ .
3. The concentrations of  $^{154}\text{Eu}$ ,  $^{155}\text{Eu}$  and  $^{241}\text{Am}$  in the organic extract decreased at the MOX feed stage, presumably because they were displaced by the extracted U and Pu.
4. The DFs for  $^{134}\text{Cs}$  and  $^{137}\text{Cs}$  imply that aqueous phase entrainment was <0.1 volume%, assuming that these nuclides were carried over into the organic product by entrainment of aqueous MOX feed. This assumption is supported by visual observation of the collected samples, where no entrainment could be seen.
5. The MOX scrub process resulted in about 7% of the feed U and 8% of the feed Pu being scrubbed into the aqueous phase.
6. The apparent DFs for the scrub process were >600 for  $^{244}\text{Cm}$ , 47  $^{154/155}\text{Eu}$ , 15 for  $^{134/137}\text{Cs}$  and about 4 for  $^{241}\text{Am}$ .
7. The concentrations of the fission products did not decrease by a large factor over the first four scrub stages. This might be due to significant entrainment between the stages although this was observed only in the case of two samples of the interstage aqueous phase.
8. Alternatively, it is possible that a high proportion of entrained micro-drops of MOX solution in the organic feed were not effectively removed by most of the scrub stages.

---

This work was performed by Summit AEA Corporation under contract with Japan Nuclear Cycle Development Institute.

JNC Liaison: Recycle process Technology Group, Advanced Fuel Recycle Technology Division, Waste Management and Fuel Cycle Research Center, Tokai Works.

\* AEA Technology

# Contents

<b>1</b>	<b>Introduction</b>	<b>1</b>
<b>2</b>	<b>Experimental method</b>	<b>1</b>
2.1	PREPARATION OF MOX FEED SOLUTIONS	1
2.2	PREPARATION OF NON-ACTIVE FEED SOLUTIONS	2
2.3	EXTRACTION EQUIPMENT	2
2.3.1	Contactors	2
2.3.2	Ancillary equipment	4
2.4	TEST PROCEDURE	5
2.4.1	Extraction	5
2.4.2	Scrub	7
2.5	CALCULATION OF DF	8
<b>3</b>	<b>Analysis</b>	<b>8</b>
<b>4</b>	<b>Results</b>	<b>9</b>
4.1	EXTRACTION	9
4.1.1	Flowrates and U, Pu and nitric acid concentrations of feeds and products	9
4.1.2	U,Pu and nitric acid concentrations in interstage samples	11
4.1.3	Concentrations of the fission products and minor actinides	12
4.1.4	Calculated DF's from fission products and minor actinides	13
4.2	SCRUB	14
4.2.1	Flowrates, U, Pu and nitric acid concentrations of feeds and products	14
4.2.2	U,Pu and nitric acid concentrations in interstage samples	14
4.2.3	Concentrations of the fission products and minor actinides	16
4.2.4	Calculated DF's from fission products and minor actinides	17
4.3	OBSERVATIONS ON DISMANTLING EQUIPMENT	17
<b>5</b>	<b>Conclusions</b>	<b>18</b>
<b>6</b>	<b>References</b>	<b>18</b>
<b>Appendices</b>		
	APPENDIX 1 FIGURES	app-1 (19)
	APPENDIX 2 PHOTOGRAPHS	app-6 (24)

# 1 Introduction

JNC are interested in the Purex liquid-liquid extraction process for the reprocessing part of an advanced nuclear fuel cycle.

Centrifugal contactors offer the following potential advantages for liquid-liquid extraction;

- compact plant and therefore potentially lower capital and operating costs
- reduced contact times between the liquid phases, therefore less solvent degradation due to radiolysis and lower volumes of waste from solvent clean-up operations
- relatively low liquid inventories which, combined with short residence times, give rapid start up, shutdown and wash out of the equipment, for example for nuclear material accounting.

This report gives the results of extraction and scrub tests with miniature centrifugal contactors, that were performed on irradiated MOX fuel containing approximately 10% Pu. Due to the highly radioactive nature of this material the experiments were performed in a hot-cell.

## 2 Experimental method

### 2.1 PREPARATION OF MOX FEED SOLUTIONS

The initial MOX fuel solution was prepared by dissolution of MOX fuel in Zircaloy cladding. Several fuel pins were cut into about 25mm lengths using a pipe cutter and loaded into a stainless steel basket. The stainless steel basket was then lowered into a dissolution vessel containing 9.5M HNO<sub>3</sub>. The lid of the vessel was clamped into place and the solution heated to ~100°C by means of an electrical band heater. During dissolution, the NO<sub>x</sub> fumes produced passed through a condenser attached to the lid and then through an engineered scrubber.

The dissolution was allowed to proceed for 8 hours and then the heater turned off. Once the solution had cooled it was pumped to an interim storage bottle and then filtered under vacuum through a 0.45µm microfilter.

A total of three dissolutions were performed and the resulting product diluted with nitric acid to produce about 3.2 litres of solution. The solution was analysed by UV/vis spectrophotometry for U and Pu, and also by titration for acidity, and found to contain  $237 \pm 12$ gU/l and  $24 \pm 2$ gPu/l, and  $4.7 \pm 0.2$ M HNO<sub>3</sub>. Photographs of the product solution and undissolved residues were taken and provided to JNC with the report on crystallisation<sup>(1)</sup>.

Approximately 500ml of the MOX solution were removed and processed to produce a solution suitable for crystallisation tests described in AEAT/NS/R/0532. The remainder of the MOX solution was stored for approximately 3 months for the extraction and scrub tests. One day before the extraction and scrub tests, a sample of MOX solution was removed from the bottom of the storage container. There was no visible evidence of any particles in the solution i.e. insoluble fuel residues, which has not been filtered out, or precipitates formed during the period of storage. The sample was re-analysed by UV-vis spectrophotometry and found to contain  $255 \pm 13\text{gU/l}$  and  $24 \pm 2\text{gPu/l}$ . There was no evidence of any Pu(VI) in the solution, as shown by the spectrophotometer scan in Figure 1. (The wave length for Pu(VI) is about 830nm, as the spectrum in Figure 2 shows).

The high-active organic product from the extraction test was used as quickly as possible as the feed to the scrub test. This action was taken to minimise the coalescence and settling out of the micro-drops of aqueous phase entrained in the organic product, since these drops are the main mechanism by which insoluble fission products such as Cs are carried over into the product. The organic feed to the scrub was therefore as representative as possible of the feed to an actual scrub process.

The time between finishing extraction and starting scrubbing was approximately 4 hours, due to the time needed to change the configuration of the ancillary equipment, as explained in Section 2.3.2.

## **2.2 PREPARATION OF NON-ACTIVE FEED SOLUTIONS**

Approximately 5 litres of a solution of 30volume% tri-n-butyl phosphate (TBP) in n-dodecane (nD) was prepared by adding sufficient nD to 1.5 litres of TBP to make up the required total volume. The TBP/nD solution was cleaned and conditioned in four stages, as follows:

- (i) clean with an equal volume of 0.1M NaOH
- (ii) clean with an equal volume of 0.1M Na<sub>2</sub>CO<sub>3</sub>
- (iii) rinse two times with 50% volume of water
- (iv) pre-condition with an equal volume of 0.1M HNO<sub>3</sub>.

The density of the solvent after step (iii) was measured to be 0.8240g/ml, which is close to the value of 0.8255g/ml for water-saturated 30%TBP/nD given in the TBP Handbook<sup>(2)</sup>.

Scrub acid was made up by diluting analytical grade concentrated nitric acid with pure water. The concentration of the scrub acid was measured by titration with 0.1M sodium hydroxide solution using phenolphthalein indicator.

## **2.3 EXTRACTION EQUIPMENT**

### **2.3.1 Contactors**

Six miniature BXP 012 centrifugal mixer settlers were supplied by Rousselet/Robatel which specialises in solid-liquid and liquid-liquid extraction equipment.

Each contactor mixes the aqueous and solvent phases in the annulus between a hollow rotor and stationary bowl. The mixture is then drawn into the rotor, by the pumping effect of vanes

machined into the bottom of the bowl, and the liquids separated under the centripetal force. The separated liquid phases pass over internal weirs and into collector galleries from where they flow by gravity to the next stage. (The dimensions of the internal weirs have an effect on the position of the liquid mixture inside the rotor and hence the phase-separation performance of the contactor, and were designed by Rousselet/Robatel for nuclear fuel reprocessing). The rotor motor is mounted on top of a block containing the coupling between the rotor shaft and the motor shaft.

The BXP 012 rotor assembly is shown in Photograph 1. The rotor is 12mm diameter and it and all other wetted parts are made of 316L stainless steel. The exception to this material are the 'O'-ring gaskets, which seal the aqueous weir from the organic weir inside the rotor, and the binding pieces and bowls, which are made of Kalrez<sup>®</sup> and was chosen by the supplier because of its high radiation resistance.

The BXP 012 bowl is viewed from above in Photograph 2, which shows the vanes at the bottom of the bowl and the galleries for collecting the two liquid phases halfway up. One of the two pins, which locate in recesses in the rotor assembly, can be seen on the bottom right-hand side of Photograph 2.

The assembled rotor and bowl are shown in Photograph 3. The outlet ports in the bowl for the aqueous phase (smaller diameter port) and the organic phase (larger diameter port) can be seen. Also, along the side of the bowl is a machined recess so that the bowl can be slid along a support rail, as described below.

Photograph 4 gives a close-up of a binding piece and shows the two 'O'-rings which fit into recesses around the liquid transfer ports and seal the binding pieces and the two adjacent bowls. Two holes are drilled down through the binding piece to the liquid transfer ports to ensure that the system is open to atmospheric pressure. The holes also provide an opportunity for interstage liquid sampling and two tubes at the top of the binding pieces help locate a sampling device in the holes. In the case of the binding pieces at the ends of the set of contactors, one of the liquids is fed via one tube while the other phase flows out by a hole and tube under the other tube.

The six contactors are mounted on a support rail as shown in Photograph 5. The rotor/bowl assemblies slide onto the rail from left to right, the binding pieces are slotted in between the bowls and then all the components are clamped together. The motor housing is then located on a rotor assembly with a large central 14mm pin and 'O' ring, and the same type of peripheral pin used with the rotor and bowl. The main central pin and 'O' ring and a peripheral pin can be seen at the top of the rotor/bowl assembly in Photograph 3. At the ends of the rotor and motor shafts are couplings held fast on the shafts by grub screws. Two pins at the end the motor coupling drive two similar pins on the rotor coupling. Photograph 6 is the underside of a motor and shows the recesses for the main central 14mm pin and the peripheral pins on the rotor assembly, and the two drive pins on the motor coupling.

The contactors were designed by Rousselet/Robatel so that the more dense aqueous phase is fed into the tube on front of the right-hand side of the assembly, stage 6, and passes to the exit of the left-hand side, stage 1. Conversely, the organic phase is fed into the tube at the back of the left-hand side, stage 1, and passes counter-currently to stage 6 on right-hand side.

The motors are 24 V direct current, encased in machined stainless steel, which fit onto the rotor assemblies as described above. The speed of each motor is controlled individually, by a potentiometer and speed display unit as shown on Photograph 7 of the control panel. Speed is measured by a tachometer on the motor shaft and the tachometer signal is fed back to an automatic PID control system to ensure constant speed.

### **2.3.2 Ancillary equipment**

The liquids were fed to the contactors with FMI 'Labpump' type QG20 metering pumps. These pumps have ceramic pistons that reciprocate with a constant time period. Flowrate is adjusted with a screw that varies the displacement of the piston. The piston setting was read from a 'coarse' scale by the pump head and also a 'fine' scale given by a vernier, as shown on Photograph 8.

The process tubing was made as flexible as possible to simplify assembly in the hot cell and enable arrangements to be changed quickly from extraction to scrub. The piston casing and process tubing for the MOX feed were made of stainless steel. The piston casing and process tubing for the non-active organic and scrub feeds were made of polyvinylidene difluoride (pvdf) and polytetrafluoroethylene (ptfe) respectively.

Samples of the liquids flowing between the contactor (i.e. the 'interstage' samples) were taken with syringe tools suited to telemanipulator operation. Robust stainless steel syringe needles, with an engineered coupling ('luer') for attaching to the syringe barrels, were inserted into the guide tubes in the binding pieces. In the case of the extraction test, the syringe tools were set up in the sampling tubes before starting the experiment, because of the demand for frequent sampling. Since the needles were 2mm diameter, it was necessary to hold them up with steel clips to avoid blocking the liquid transfer ports, and to release a clip and lower a needle when the sample was required. A needle and clips are shown, with a binding piece, in Photograph 4. In the case of the scrub test, samples were required less frequently and therefore the sampling tool was inserted into the guide tube when the sample was required.

The syringe barrels were 'Luer Lok' Series 1000 made by Hamilton – Bonaduz. The barrels were gas-tight so that they could be disconnected from the needles and stored temporarily without any loss of liquid. Photograph 9 shows a syringe barrel being manipulated in the hot cell.

The arrangement of the ancillary equipment for extraction is shown in Figure 3. Non-active organic feed was pumped to the stage 1 end of the contactor assembly. The organic product flowed from stage 6 initially to a uranium-active product vessels and then to a high-active product vessel. The valve system enabled samples of the organic product to be taken directly, via valve SV2, during the test. The aqueous feed was pumped to the stage 6 end of the contactor assembly.

An arrangement of valves enabled initial start up with 2M nitric acid, then 250gU/l in 4.7M nitric acid (to simulate the MOX feed as closely as possible) and finally MOX feed. The aqueous raffinate flowed from stage 1 initially to an uranium-active raffinate vessel and then to a high-active raffinate vessel. Valve SV1 enabled the flowrate of aqueous raffinate to be measured during the non-active and U-active start-up phase. At the end of the MOX test,

feeds reverted to 2M nitric acid and non-active solvent, with the product and raffinate diverted to the uranium-active vessels, for five minutes to rinse the equipment of active liquids. The change-over of the aqueous feeds and product and raffinate valves was timed to minimise any dilution of the collected high-active product and high-active raffinate.

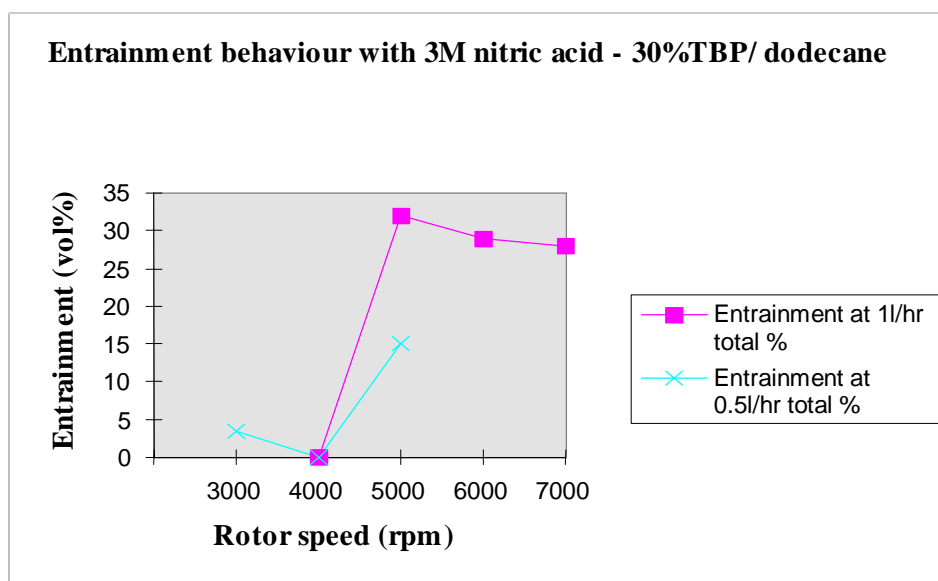
The arrangement of the ancillary equipment for scrub is shown in Figure 4. The same pump that had been used to feed non-active organic phase was used to feed 2M nitric scrub acid, to the stage 6 end, in order to minimise contamination of the acid feed. The organic feed was pumped to the stage 1 end of the contactor assembly and the valves used to start up initially on uranium-active organic feed and then to process the high-active organic phase collected from the extraction test. The other valve systems were used to direct the aqueous raffinate and scrubbed organic product between uranium-active and high-active vessels as required by the start-up and final rinse procedures.

## 2.4 TEST PROCEDURE

### 2.4.1 Extraction

The in-cell temperature was checked with a digital thermometer immediately before and after the test.

The contactors were then started up at 4000rpm, which earlier tests with acid and uranium solutions in a fume cupboard had shown was the optimum. This is illustrated by the data below.



An aqueous feed of 2M nitric acid and an organic feed of 30%TBP/nD were switched on and the contactors were operated on these liquids for about an hour to check that conditions were stable. In particular, the flowrates of the aqueous and organic feeds were measured by collecting samples from valves SV1 and SV2 with measuring cylinders, and the samples checked for any evidence of entrainment.

The aqueous feed was then switched from 2M nitric acid to 250 gU/litre in 4.7M nitric acid and operated in this mode for an hour to re-check that conditions were stable. In particular, the aqueous raffinate was inspected for any visible evidence of uranium breakthrough, and the organic product and aqueous raffinate were checked for any evidence of entrainment of one phase in the other. No uranium breakthrough or entrainment were seen. The flowrates of the aqueous and organic phases were measured by taking samples of the liquids exiting the end stages in measuring cylinders.

The feeds and contactors were then switched off over-night. The following morning the equipment was restarted with UN/nitric acid and organic feeds and operated for 30 minutes in this mode to re-check flowrates and performance. The aqueous feed was then switched to active MOX solution and operated in this mode for about 3.5 hours. This was somewhat longer than planned because of difficulty in taking one of the interstage samples. During the 3.5 hours, six samples of organic product, that exits from contactor 6, were taken from valve SV2 and eight interstage samples were taken with syringe tools at the following times.

**Table 1. Sample schedule for MOX extraction test**

<b>Sample</b>	<b>Approximate time after start-up of MOX feed* (mins)</b>
Organic exit of contactor 6	30
Interstage aqueous 2-3	46
Organic exit of contactor 6	60
Interstage aqueous 3-4	62
Interstage aqueous 4-5	93
Organic exit of contactor 6	97
Interstage aqueous 5-6	118
Organic exit of contactor 6	122
Interstage organic 5-6	140
Organic exit of contactor 6	147
Interstage organic 4-5	161
Interstage organic 3-4	179
Organic exit of contactor 6	186
Interstage organic 2-3	199

\*Note: in the case of the interstage samples, this is the mid-point of starting and finishing sampling (which took 2 to 5 minutes)

At the end of the 3.5 hours operation on MOX feed, a check was made that all the samples listed above have been taken. The aqueous feed was then switched from MOX to 2M nitric acid and the contactors rinsed with non-active feeds for 20 minutes.

The collected high-active organic product exiting from contactor 6 was sampled from the high-active organic product vessel. The collected high-active aqueous raffinate exiting from contactor 1 was sampled from the high-active aqueous raffinate vessel.

The equipment was then re-configured for the scrub test, as described in the previous Section. The collected high-active aqueous raffinate and high-active organic product vessels were inspected for entrainment and none was evident.

During the test, the following information was recorded in the experimental logbook:

- frequent readings of rotor speed
- observations of the contactors and interconnecting ports to ensure liquid is not overflowing from a contactor
- observations of the status of the contactor parts, taking photographs during and after the tests.

A video recording was made of the whole duration of the test.

#### **2.4.2 Scrub**

The in-cell temperature was checked with a digital thermometer immediately before and after the scrub operation.

The contactors were then started up at 4000rpm, with an aqueous feed of 2M nitric acid and an organic feed of the uranium-active organic solution collected during the start-up of the extraction process. The contactors were operated on these liquids for just over an hour to check that conditions were stable. In particular, the flowrates of the aqueous and organic feeds were measured by collecting samples from valves SV1 and SV2 with measuring cylinders, and the samples were checked for any evidence of entrainment. The scrub acid exiting stage 1 and the organic product exiting stage 6 were sent to the U-active aqueous raffinate vessel and the U-active organic product vessel respectively.

The organic feed was then switched to the high-active organic solution produced by extraction and operated in this mode for about three hours. During this time the following interstage samples were taken.

**Table 2. Sample schedule for MOX scrub test**

<b>Sample</b>	<b>Approximate time after start-up of MOX feed* (mins)</b>
Interstage aqueous 1-2	20
Interstage aqueous 2-3	47
Interstage aqueous 3-4	73
Interstage organic 4-5	98
Interstage organic 3-4	125
Interstage organic 2-3	150
Interstage organic 1-2	176

\*Note: sampling took between 1 and 2 minutes, and the time that sampling was started is shown.

After terminating the high-active feed, the equipment was rinsed for 15 minutes with scrub acid, and the scrub acid exiting stage 1 was sent to the U-active aqueous raffinate vessel. During this time, samples were taken of the collected scrubbed organic product that exited from contactor 6, from the high-active organic product vessel, and the collected active aqueous raffinate from contactor 1, in the high-active aqueous raffinate vessel.

## 2.5 CALCULATION OF DF

All DFs are calculated with respect to the mass of U.

The DFs for the measured fission products,  $^{241}\text{Am}$  and  $^{244}\text{Cm}$ , are calculated from the radioactivity of these species, i.e.

$$\text{DF} = \frac{\text{Bq/g U in the MOX feed solution}}{\text{Bq /g U in the product solution}} \quad (1)$$

## 3 Analysis

The following analytical techniques were applied to the samples.

- a) U in concentrations above 0.5g/l and Pu in concentrations above 0.05g/l, and Pu valence, were measured by UV/visible spectrophotometry. This technique required a 0.1ml aliquot of process solution to be taken with a pre-calibrated Gilson<sup>®</sup> pipette, and diluted with 3mls or 5mls of 6M nitric acid to be within the range of the instrument. The nitric acid was dispensed from a stock solution with a 1ml capacity Gilson<sup>®</sup> pipette. The overall precision of this technique is  $\pm 5\%$  for the concentrations measured, including dilution errors.
- b) Nitric acid concentration was determined by titrating a sample of solution, buffered with potassium fluoride to complex U and Pu, with 0.1M sodium hydroxide solution using phenolphthalein indicator. For the aqueous phase, the 1ml capacity Gilson<sup>®</sup> pipette was used to dispense the initial quantities of sodium hydroxide solution and the 0.1ml capacity Gilson<sup>®</sup> pipette to dispense the quantities when close to the end point. The overall precision of the technique for the aqueous phase is  $\pm 0.2\text{M}$ . For the organic phase, the smaller pipette was used throughout titration and precision of the technique was  $\pm 0.1\text{M}$ .
- c) Pu in concentrations below about 0.05g/l was analysed by alpha spectrometry. An aliquot of the solution prepared for UV/visible spectrophotometry was further diluted so that it could be safely posted from the hot cell into a fume cupboard, for preparation of a dried film for alpha counting. The 0.1mm Gilson<sup>®</sup> pipette and calibrated volumetric flasks were used for this purpose. In the case of very low Pu concentrations,  $^{241}\text{Am}$  was first removed by solvent extraction so that it would not interfere with the analysis. The technique was to dilute the sample with 8M HCl, extract the Pu (and U) into tri-iso-octylamine (TOA) and then strip the Pu (and U) into dilute acid for electrodeposition of a thin film onto the counting tray. A known quantity of  $^{236}\text{Pu}$  tracer was added to the untreated sample so that the yield of purified Pu given by the solvent extraction process could be calculated. The total Pu in the sample was calculated from the  $^{239}\text{Pu}/^{240}\text{Pu}$  detected by alpha counting from the known isotopic composition of the Pu (1.596wt%  $^{238}\text{Pu}$ , 54.584wt%  $^{239}\text{Pu}$ , 32.456wt%  $^{240}\text{Pu}$ , 5.241wt%  $^{241}\text{Pu}$ , 6.123wt%  $^{242}\text{Pu}$ ).

- d) U in concentrations below about 0.5g/l was also analysed by alpha spectrometry. In this case,  $^{241}\text{Am}$  and Pu were first removed by solvent extraction so that they would not interfere with the analysis. The same initial procedure was followed as for Pu in c) above. The Pu was then stripped from the TOA with a solution of ammonium iodide in HCl and the U stripped into dilute acid for electrodeposition onto the counting tray. A known quantity of  $^{233}\text{U}$  tracer was added to the untreated sample so that the yield of purified U given by the solvent extraction process could be calculated. The total U in the sample was calculated from the known isotopic composition of the U (0.015wt%  $^{234}\text{U}$ , 0.428wt%  $^{235}\text{U}$ , 0.041wt%  $^{236}\text{U}$  and 99.517wt%  $^{238}\text{U}$ ).
- e) The main fission products,  $^{134}\text{Cs}$ ,  $^{137}\text{Cs}$ ,  $^{154}\text{Eu}$ ,  $^{155}\text{Eu}$  and  $^{241}\text{Am}$  were detected by gamma spectrometry. Although it was not possible to detect  $^{144}\text{Ce}$  or  $^{106}\text{Ru}$  by this technique, as they had decayed due to their relatively short half-life, it was possible to detect  $^{125}\text{Sb}$ , although the higher error on the analysis of this nuclide results in less accurate mass balances. The solution was diluted and prepared for counting as described in c) above.
- f) Samples of solution were analysed for  $^{244}\text{Cm}$  by alpha spectrometry. Where Pu was present in large concentrations, Pu was first removed from the sample by the separation technique described in c) above.

In the case of the organic samples, the U, Pu and fission products needed to be stripped into an aqueous phase for analysis. In the case of the organic product samples taken during extraction for U and Pu analysis, an aliquot of the sample was taken and stripped with a 5x excess of 0.25M sulphuric acid, and then further diluted to bring concentration within the range of UV-vis. In the case of the interstage organic samples and collected organic product, it was important to ensure that all the entrained aqueous drops, which might have coalesced on the wall of the sample container and the syringe barrel, were captured in the final stripped sample. Therefore a syringe barrel was rinsed with acid which was added to the bulk sample, with further acid to obtain the overall 5x excess.

## 4 Results

### 4.1 EXTRACTION

#### 4.1.1 Flowrates, and U, Pu and nitric acid concentrations in products

The flowrates and U, Pu and nitric acid concentrations of the feeds and products are shown in Table 3 below. The flowrates are based on the pre-run measurements, where appropriate, and the change in volume in the vessels measured over the whole test. The temperature measured just before the test began was 21.7°C and immediately after the test was completed was 23.3°C.

**Table 3 Flowrates, U, Pu and nitric acid concentrations in feeds and products for MOX extraction, mean temperature of 22.5°C**

Solution	Flowrate (mls/hr)		Concentrations		
	Measured before test	From volume change in vessel <sup>1</sup>	U (g/l)	Pu (g/l)	Nitric acid (M)
MOX feed	250 <sup>2</sup>	270	246 <sup>3</sup>	24	4.7
Organic feed	768 <sup>4</sup>	740	-	-	0.1
High-active organic product	-	770	85.8	8.58	0.5
High-active aqueous raffinate	-	240	2.11E-02	1.39E-03	4.1

- Notes:
1. These data are rounded to the nearest 10mls/hr.
  2. Flowrate of MOX feed is average of three measurements of collected aqueous raffinate during operation with UN feed.
  3. Average of two measurements by UV-visible spectrophotometry, made about two months apart.
  4. Flowrate of organic feed is average of five measurements of collected organic product, two with nitric acid and organic feeds and three with UN/nitric acid and organic feeds.

The concentrations of U and Pu in the high-active aqueous raffinate show that >99.99% of both actinides were recovered by the extraction process.

Photograph 10 gives a view of the equipment towards the end of the extraction test. The high-active product appears to be a dark blue-green, and the high-active aqueous raffinate to be a light yellow-brown, under the lighting conditions in the hot cell.

The concentrations of U and Pu in the six samples of organic product are given in Table 4 below. The mean and standard deviations are 80.13g/l  $\pm$  2.18g/l for U and 7.79g/l  $\pm$  0.89g/l for Pu. The standard deviation for U is about 3% of the mean.

**Table 4 U and Pu concentrations in organic product from MOX extraction**

Sample	Time taken after MOX feed start up	Concentrations (g/l)	
		U	Pu
1	30	75.6	6.75
2	60	85.0	9.25
3	97	85.3	7.25
4	122	81.5	7.50
5	147	81.1	8.25
6	186	72.3	7.75

The U and Pu concentrations in the collected high-active organic product (85.8g/l and 8.58g/l respectively) are higher than the average of the six samples taken during the run. However, the Pu concentration in the collected high-active organic product measured by UV-visible spectrophotometry was confirmed by alpha spectrometry (8.52g/l by alpha spectrometry compared with the 8.58g/l by UV-visible spectrophotometry).

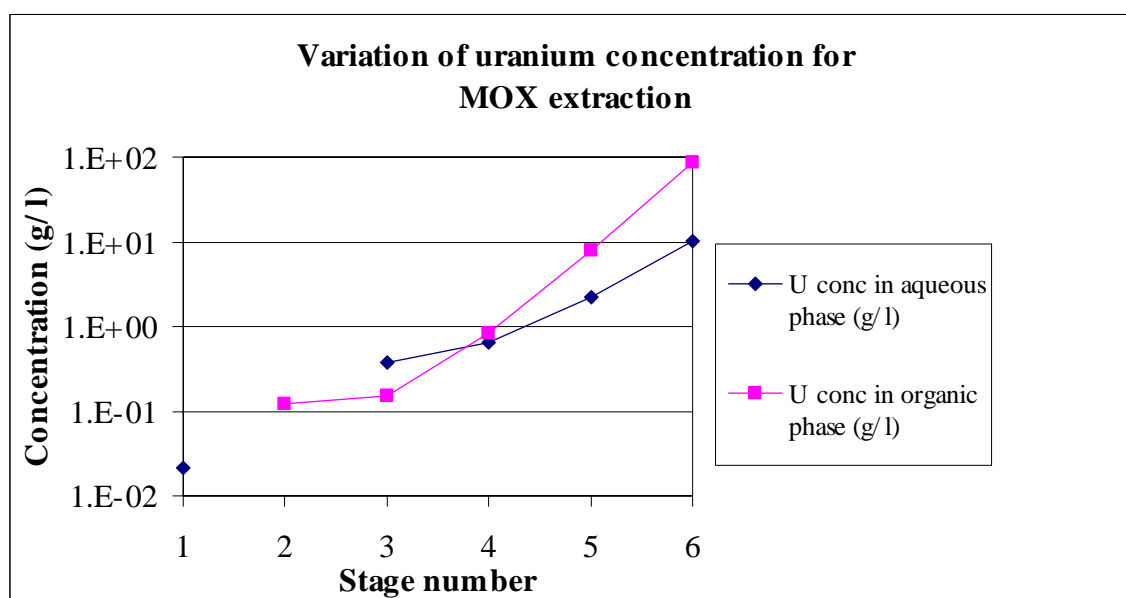
#### 4.1.2 U, Pu and nitric acid concentrations in interstage samples

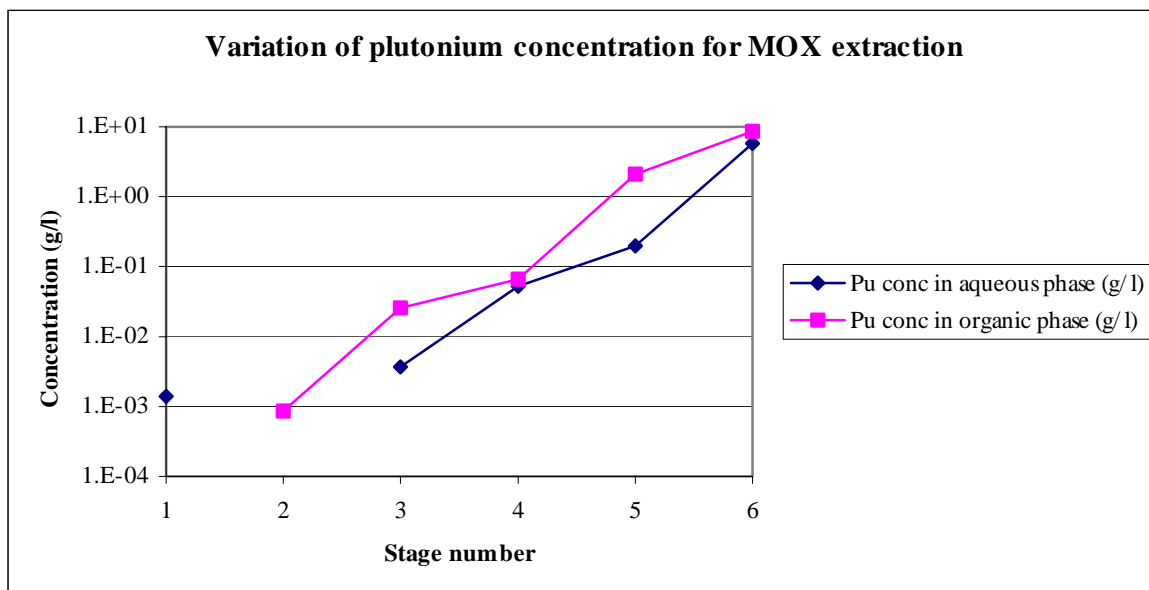
The U, Pu and nitric acid concentrations in the interstage samples are given in Table 5. Please note that there was no evidence of any entrainment in the interstage samples.

**Table 5 U, Pu and nitric acid concentrations in interstage samples from MOX extraction**

Sample	Concentrations		
	U (g/l)	Pu (g/l)	Nitric acid (M)
Interstage 5-6 organic	8.02	2.09	0.5
Interstage 4-5 organic	8.46E-01	6.65E-02	1.1
Interstage 3-4 organic	1.54E-01	2.55E-02	1.1
Interstage 2-3 organic	1.20E-01	8.55E-04	1.0
Interstage 5-6 aqueous	10.3	5.83	5.7
Interstage 4-5 aqueous	2.2	1.97E-01	5.5
Interstage 3-4 aqueous	6.41E-01	5.20E-02	5.8
Interstage 2-3 aqueous	3.76E-01	3.67E-03	5.9

The following Figures plot the data in Table 5 as the concentrations in the aqueous and organic phases leaving each stage.





It can be seen from Table 5 that the nitric acid concentration in the organic phase was about 1.0M to 1.1M where U and Pu concentrations were low and decreased to 0.5M towards the MOX feed stage due to U and Pu extraction. This caused the nitric acid concentration in the aqueous phase along the contactors to be higher than in the MOX feed and collected aqueous raffinate from stage 1 i.e. on average 5.7M along the contactor bank compared with 4.7M and 4.1M in the MOX feed and aqueous raffinate respectively.

#### 4.1.3 Concentrations of the fission products and minor actinides

The concentrations of  $^{241}\text{Am}$ ,  $^{244}\text{Cm}$ ,  $^{134}\text{Cs}$ ,  $^{137}\text{Cs}$ ,  $^{154}\text{Eu}$ ,  $^{155}\text{Eu}$  and  $^{125}\text{Sb}$  in the samples are given in Table 6 below.

**Table 6. Concentrations of fission products and minor actinides for MOX extraction.**

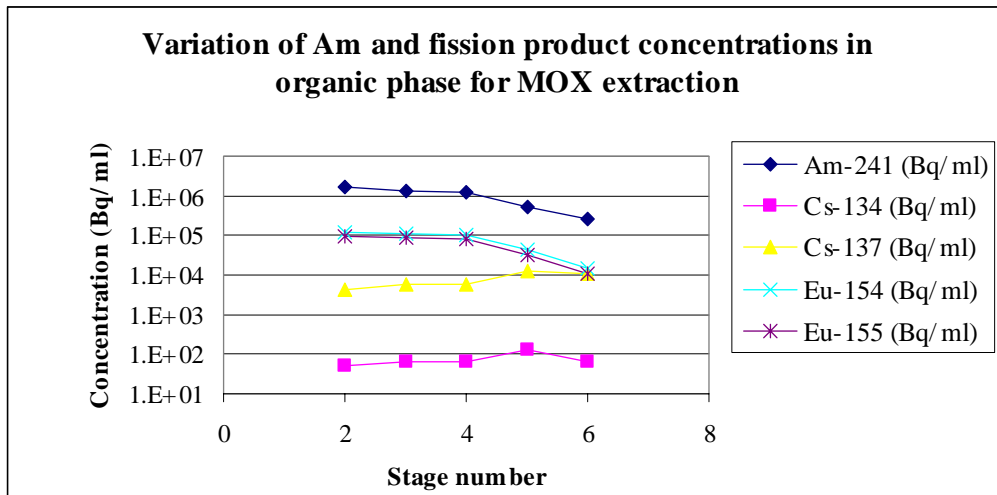
Sample	Concentrations (Bq/ml)*						
	$^{241}\text{Am}$	$^{244}\text{Cm}$	$^{134}\text{Cs}$	$^{137}\text{Cs}$	$^{154}\text{Eu}$	$^{155}\text{Eu}$	$^{125}\text{Sb}$
MOX feed solution	1.05E08	1.00E07	1.05E06	2.99E08	3.29E06	2.63E06	8.94E05
High-active aqueous raffinate	1.20E08	1.16E07	1.14E06	3.36E08	3.66E06	2.89E06	1.03E06
High-active organic product	2.61E05	2.02E04	6.37E01	1.09E04	1.44E04	1.05E04	2.26E02
Interstage 5-6 organic	5.31E05	-	1.34E02	1.24E04	4.24E04	3.27E04	<7.80E02
Interstage 4-5 organic	1.19E06	-	6.61E01	5.59E03	1.01E05	8.05E04	<1.40E02
Interstage 3-4 organic	1.32E06	-	6.38E01	5.97E03	1.10E05	8.66E04	<1.50E03
Interstage 2-3 organic	1.62E06	-	5.29E01	4.15E03	1.20E05	9.32E04	<1.20E03
Interstage 5-6 aqueous	1.07E08	-	9.75E05	2.89E08	3.39E06	2.68E06	8.35E05
Interstage 4-5 aqueous	1.17E08	-	1.05E06	3.15E08	3.77E06	2.93E06	9.59E05

Interstage 3-4 aqueous	1.16E08	-	1.08E06	3.08E08	3.79E06	2.98E06	9.44E05
Interstage 2-3 aqueous	1.23E08	-	1.09E06	3.23E08	4.09E06	3.33E06	9.49E05

\*Note: precision of analysis is generally approximately between  $\pm 1\%$  and  $\pm 3\%$  except for  $^{125}\text{Sb}$ .

The concentrations of  $^{241}\text{Am}$ ,  $^{134}\text{Cs}$ ,  $^{137}\text{Cs}$ ,  $^{154}\text{Eu}$  and  $^{155}\text{Eu}$  in the organic phase from each stage are shown below. In the case of  $^{241}\text{Am}$ ,  $^{154}\text{Eu}$  and  $^{155}\text{Eu}$ , the concentrations in the organic phase decrease towards MOX feed stage 6 presumably because they are dissolved in the organic phase and are displaced to some extent by the extracted U and Pu.

In the cases of  $^{134}\text{Cs}$  and  $^{137}\text{Cs}$ , the concentrations in the organic phase are not affected by the extraction of U and Pu, presumably because they are present in aqueous phase entrained in the organic phase. For  $^{137}\text{Cs}$ , the average concentrations in the aqueous and organic phases along the contactors are  $3.1\text{E}+08$  and  $7.8\text{E}+03$  respectively. These data imply an average of about  $2.5\text{E}-03$  vol% entrainment of aqueous phase in the organic phase, assuming that no  $^{137}\text{Cs}$  is dissolved in the organic phase. (A similar calculation for  $^{134}\text{Cs}$  implies about  $6\text{E}-03$  vol% entrainment, which is reasonably consistent given the variation in the data).



#### 4.1.4 Calculated DFs from fission products and minor actinides

The overall DFs for the extraction process, based on the MOX feed and collected organic product from stage 6 and calculated from equation (1), are given in Table 7.

**Table 7. DFs for main elements for MOX extraction test.**

Sample	DF's						
	$^{241}\text{Am}$	$^{244}\text{Cm}$	$^{134}\text{Cs}$	$^{137}\text{Cs}$	$^{154}\text{Eu}$	$^{155}\text{Eu}$	$^{125}\text{Sb}$
Collected high-active organic product	140	173	5750	9567	80	88	1380

There is good consistency between the DF's for  $^{241}\text{Am}$  and  $^{244}\text{Cm}$ ,  $^{134}\text{Cs}$  and  $^{137}\text{Cs}$ , and  $^{154}\text{Eu}$  and  $^{155}\text{Eu}$ .

## 4.2 SCRUB

### 4.2.1 Flowrates, and U, Pu and nitric acid concentrations in products

The flowrates and U, Pu and nitric acid concentrations of the feeds and products are shown in Table 8. The flowrates are based on the pre-run measurements, where appropriate, and the change in volume in the vessels measured over the whole test. The temperature measured just before the test began was 23.5°C and immediately after the test was completed was 23.9°C.

**Table 8 Flowrates, U, Pu and nitric acid concentrations in feeds and products for MOX scrub, mean temperature 23.7°C**

Solution	Flowrate (mls/hr)		Concentrations		
	Measured before test	From volume change in vessel <sup>1</sup>	U (g/l)	Pu (g/l)	Nitric acid (M)
High-active organic feed	747 <sup>2</sup>	720	85.8	8.58	0.5
Scrub acid feed	156 <sup>3</sup>	150	-	-	2.0
High-active organic product	-	750	83.9	7.55	0.5
High-active aqueous raffinate	-	160	26.5	3.30	2.8

1. These data are rounded to the nearest 10mls/hr.
2. Flowrate of high-active organic feed is average of two measurements of collected organic product during operation with organic UN feed.
3. Flowrate of scrub acid feed is based on a final measurement before starting high-active organic feed. The measurement followed three successive adjustments to the pump to obtain as accurate a flowrate as possible.

The analysis of the high-active aqueous raffinate shows that about 7% of the feed U and 8% of the feed Pu were scrubbed from the organic phase.

Photograph 11 gives a view of the equipment towards the end of the extraction test. The high-active aqueous raffinate is a light blue-green colour, under the lighting conditions in the hot cell, because of the U and Pu removed with the fission products.

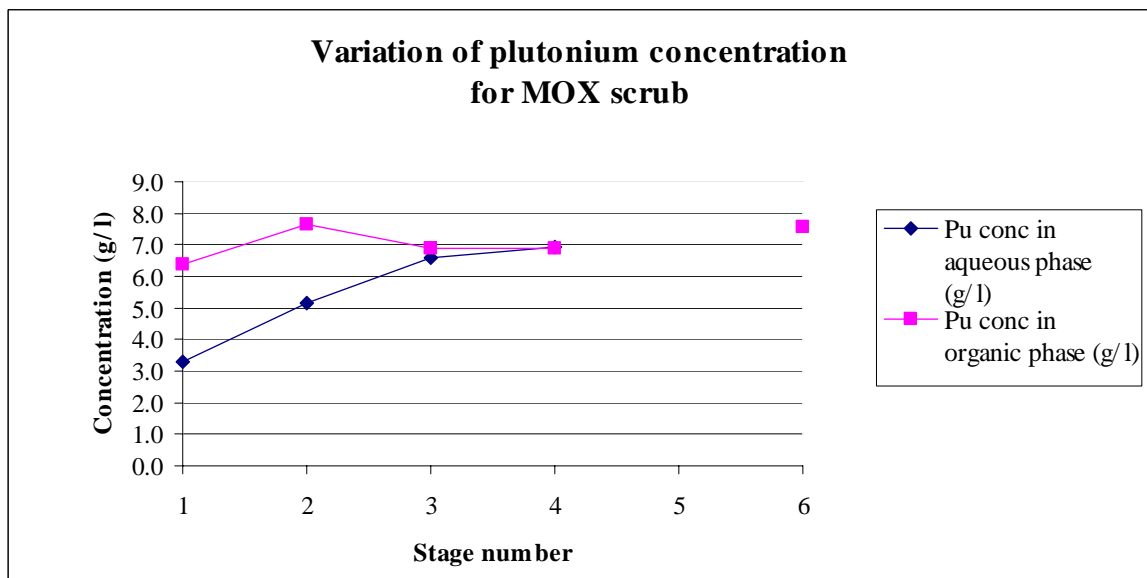
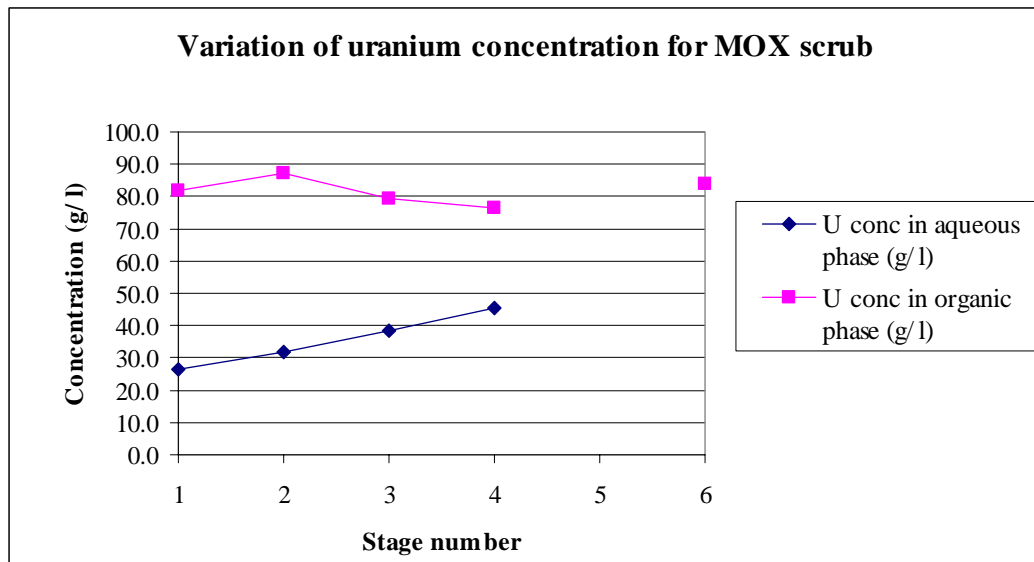
### 4.2.2 U, Pu and nitric acid concentrations in interstage samples

The U, Pu and nitric acid concentrations in the interstage samples are given in Table 9 below. Please note that interstage samples 2-3 aqueous and 3-4 aqueous contained entrained organic phase. In the case of 2-3 aqueous, about 20% on the total sample volume was organic phase. For 3-4 aqueous, the volume of entrained organic phase was too small to be measured. There was no entrainment in any of the other samples.

**Table 9 U, Pu and nitric acid concentrations in interstage samples from MOX scrub**

Sample	Concentrations		
	U (g/l)	Pu (g/l)	Nitric acid (M)
Interstage 1-2 organic	82.0	6.40	0.6
Interstage 2-3 organic	87.0	7.66	0.6
Interstage 3-4 organic	79.4	6.87	0.5
Interstage 4-5 organic	76.4	6.90	0.6
Interstage 1-2 aqueous	32.0	5.17	2.3
Interstage 2-3 aqueous	38.4	6.60	2.1
Interstage 3-4 aqueous	45.5	6.93	2.2

The following Figures plot the data in Table 9 as the concentrations in the aqueous and organic phases leaving each stage.



### 4.2.3 Concentrations for the fission products and minor actinides

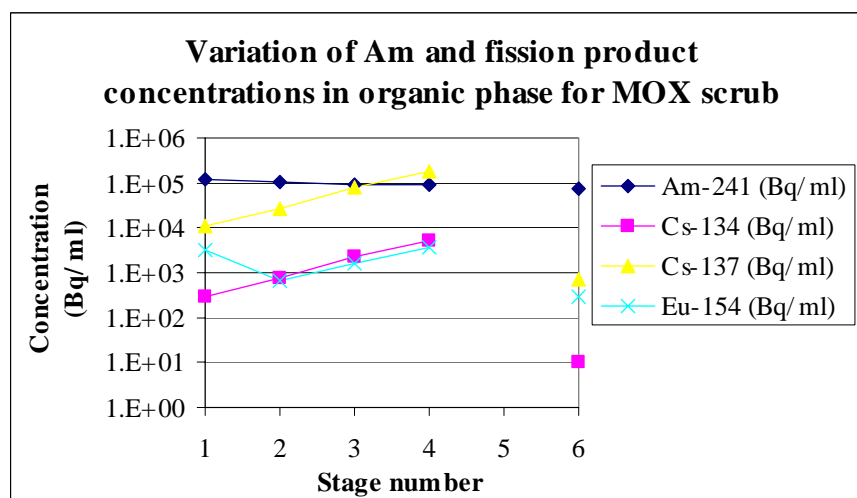
The concentrations of  $^{241}\text{Am}$ ,  $^{244}\text{Cm}$ ,  $^{134}\text{Cs}$ ,  $^{137}\text{Cs}$ ,  $^{154}\text{Eu}$ ,  $^{155}\text{Eu}$  and  $^{125}\text{Sb}$  in the samples are given in Table 10 below.

**Table 10. Concentrations of fission products and minor actinides for MOX scrub.**

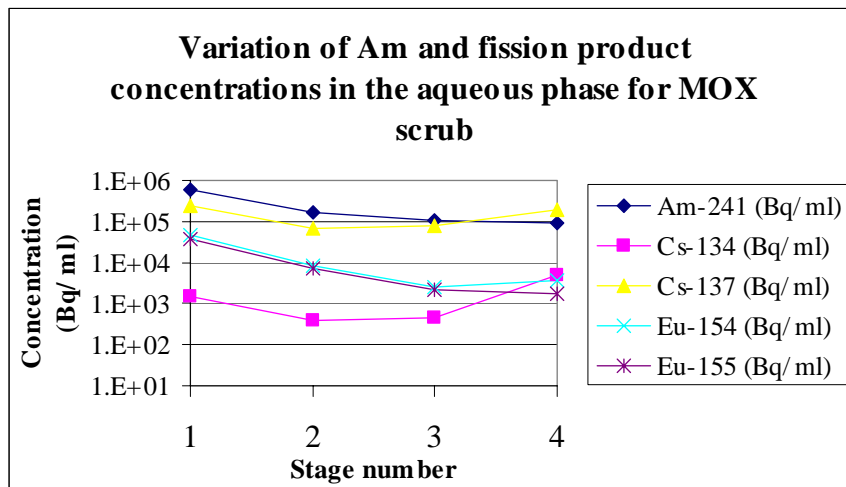
Sample	Concentrations (Bq/ml)						
	$^{241}\text{Am}$	$^{244}\text{Cm}$	$^{134}\text{Cs}$	$^{137}\text{Cs}$	$^{154}\text{Eu}$	$^{155}\text{Eu}$	$^{125}\text{Sb}$
High-active organic feed solution	2.61E05	2.02E04	6.37E01	1.09E04	1.44E04	1.05E04	2.26E02
High-active organic product solution	7.58E04	<3.0E01	1.02E01	7.08E02	<3.00E02	<7.30E03	<1.18E03
High-active aqueous raffinate	5.79E05	5.73E04	1.55E03	2.45E05	4.68E04	3.71E04	1.19E03
Interstage 1-2 organic	1.17E05	-	2.84E02	1.12E04	3.22E03	2.67E03	9.05E02
Interstage 2-3 organic	1.05E05	-	7.76E02	2.66E04	6.56E02	4.41E02	1.83E02
Interstage 3-4 organic	9.15E04	-	2.28E03	8.18E04	1.61E03	1.37E03	7.38E02
Interstage 4-5 organic	9.37E04	-	5.04E03	1.86E05	3.58E03	1.76E03	5.7E02
Interstage 1-2 aqueous	1.64E05	-	3.83E02	6.84E04	8.25E03	7.12E03	9.7E02
Interstage 2-3 aqueous	1.09E05	-	4.42E02	7.93E04	2.54E03	2.13E03	3.49E02
Interstage 3-4 aqueous	1.02E05	-	3.05E02	7.69E04	1.23E03	1.06E03	3.07E02

\*Note: precision of analysis is generally approximately between  $\pm 1\%$  and  $\pm 3\%$  except for  $^{125}\text{Sb}$ .

The concentrations of  $^{241}\text{Am}$ ,  $^{134}\text{Cs}$ ,  $^{137}\text{Cs}$  and  $^{154}\text{Eu}$  in the organic phase from each stage are shown below. ( $^{155}\text{Eu}$  is not shown because two results were below the limit of detection). In the case of  $^{241}\text{Am}$ , there is a small gradual reduction along the contactors, whilst  $^{134}\text{Cs}$  and  $^{137}\text{Cs}$  appear to increase before decreasing in the organic product from Stage 6. The  $^{154}\text{Eu}$  vary fairly randomly before decreasing in the organic product from Stage 6.



The concentrations of  $^{241}\text{Am}$ ,  $^{134}\text{Cs}$ ,  $^{137}\text{Cs}$ ,  $^{154}\text{Eu}$  and  $^{155}\text{Eu}$  in the aqueous phase from each stage are shown below. In the case of  $^{241}\text{Am}$ ,  $^{154}\text{Eu}$  and  $^{155}\text{Eu}$  there is a gradual reduction along the contactors, whilst  $^{134}\text{Cs}$  and  $^{137}\text{Cs}$  appear to vary quite randomly.



#### 4.2.4 Calculated DFs from the fission products and minor actinides

The overall DFs calculated for the scrub process, based on the concentration of the radionuclide in the high-active organic feed (Bq/gU) and that in the high-active organic product (Bq/gU) are given in Table 11 below.

**Table 11. DFs for main elements for MOX scrub test.**

Sample	DF's						
	$^{241}\text{Am}$	$^{244}\text{Cm}$	$^{134}\text{Cs}$	$^{137}\text{Cs}$	$^{154}\text{Eu}$	$^{155}\text{Eu}$	$^{125}\text{Sb}$
High-active organic product	3.4	>659	6.1	15.1	>47	NA*	NA*

\*Note: NA = not applicable because the limit of detection is too high to enable a realistic DF to be calculated.

### 4.3 OBSERVATIONS ON DISMANTLING EQUIPMENT

When the equipment was dismantled, each rotor, bowl and binding piece was examined for corrosion and deterioration of the liquid seals.

There was no evidence of any corrosion of the rotors and bowls, or deterioration of the liquid seals on the binding pieces. Photograph 12 is of the contactor and bowl for the MOX feed, stage 6. Photograph 13 is a binding piece close to the MOX feed stage. Both photographs show the good condition of the equipment.

## 5 Conclusions

The conclusions of the tests were as follows.

1. A high recovery (>99.99%) of both U and Pu were achieved by the extraction process. The performance of the contactors was very stable, as demonstrated by the variation of the U concentration in the organic product (standard deviation was  $\pm 3\%$  of the mean concentration for six samples taken during the test).
2. The DFs given by extraction were approximately between about 80 and 90 for  $^{154}\text{Eu}$  and  $^{155}\text{Eu}$ , between 140 and 170 for  $^{241}\text{Am}$  and  $^{244}\text{Cm}$ , and >1000 for  $^{134}\text{Cs}$  and  $^{137}\text{Cs}$ .
3. The concentrations of  $^{154}\text{Eu}$ ,  $^{155}\text{Eu}$  and  $^{241}\text{Am}$  in the organic extract decreased at the MOX feed stage, presumably because they were displaced by the extracted U and Pu.
4. The DFs for  $^{134}\text{Cs}$  and  $^{137}\text{Cs}$  imply that aqueous phase entrainment was <0.1 volume%, assuming that these nuclides were carried over into the organic product by entrainment of aqueous MOX feed. This assumption is supported by visual observation of the collected samples, where no entrainment could be seen.
5. The MOX scrub process resulted in about 7% of the feed U and 8% of the feed Pu being scrubbed into the aqueous phase.
6. The apparent DFs for the scrub process were >600 for  $^{244}\text{Cm}$ , 47  $^{154/155}\text{Eu}$ , 15 for  $^{134/137}\text{Cs}$  and about 4 for  $^{241}\text{Am}$ .
7. The concentrations of the fission products did not decrease by a large factor over the first four scrub stages. This might be due to significant entrainment between the stages although this was observed only in the case of two samples of the interstage aqueous phase.
8. Alternatively, it is possible that a high proportion of entrained micro-drops of MOX solution in the organic feed were not effectively removed by most of the scrub stages.

## 6 References

- (1) R Pateman, R Cooke, J Jenkins and C Mason, AEAT/R/NS/0532 " The Crystallisation of Irradiated MOX Fuel " (2002).
- (2) Science and Technology of TBP, edited by W W Schulz, L L Burger and J D Navratil, CRC Press, Boca Raton, Florida, USA (1990)

# Appendix 1

## Figures

---

### CONTENTS

Figure 1. UV-visible spectrum of MOX feed solution to extraction process	app-2 (20)
Figure 2. UV-visible spectrum showing Pu(VI) peak at 830nm	app-3 (21)
Figure 3. Equipment arrangement for extraction	app-4 (22)
Figure 4. Equipment arrangement for scrub	app-5 (23)

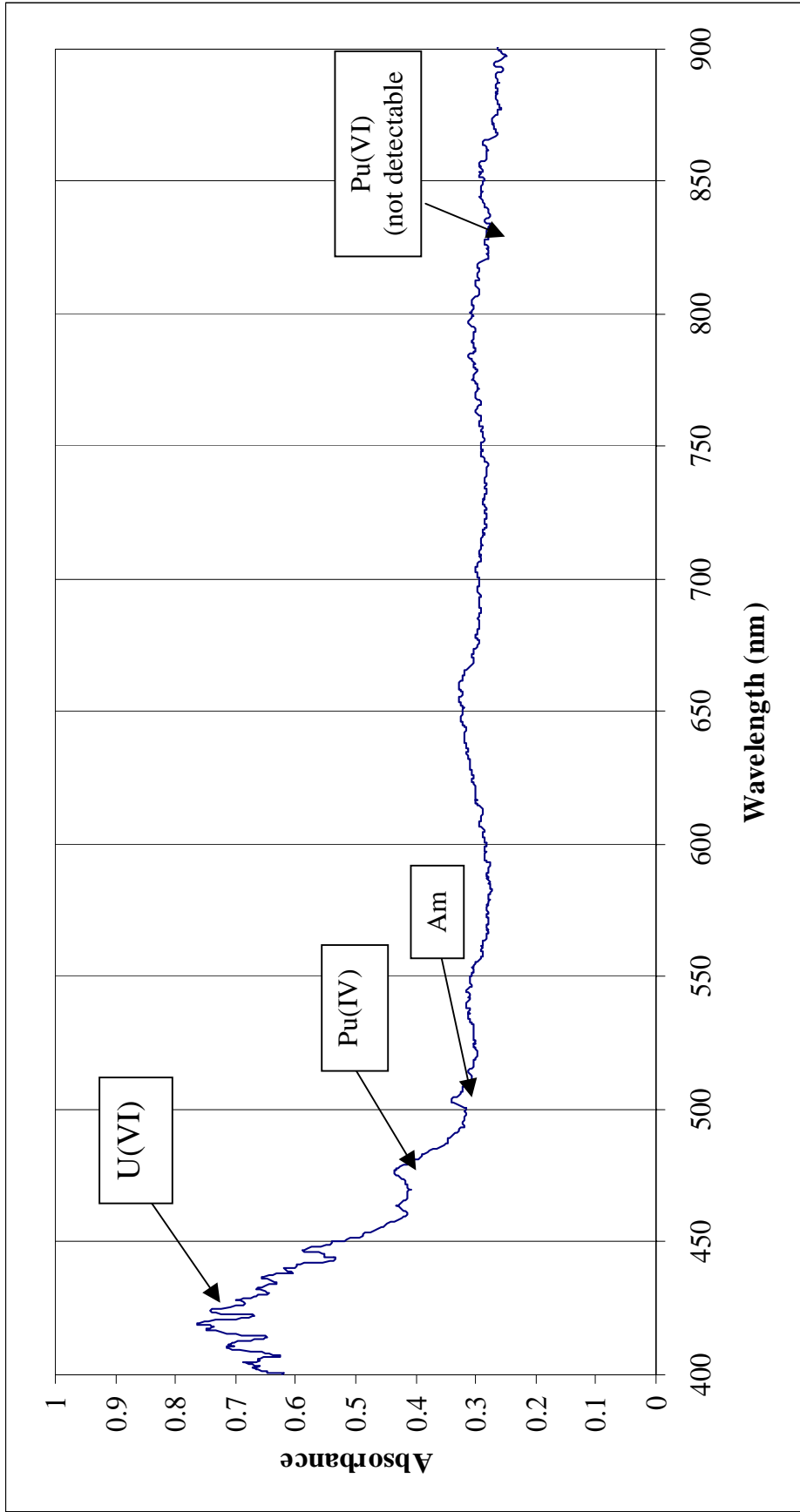


**Figure 1. UV-visible spectrum of MOX feed solution to extraction process**

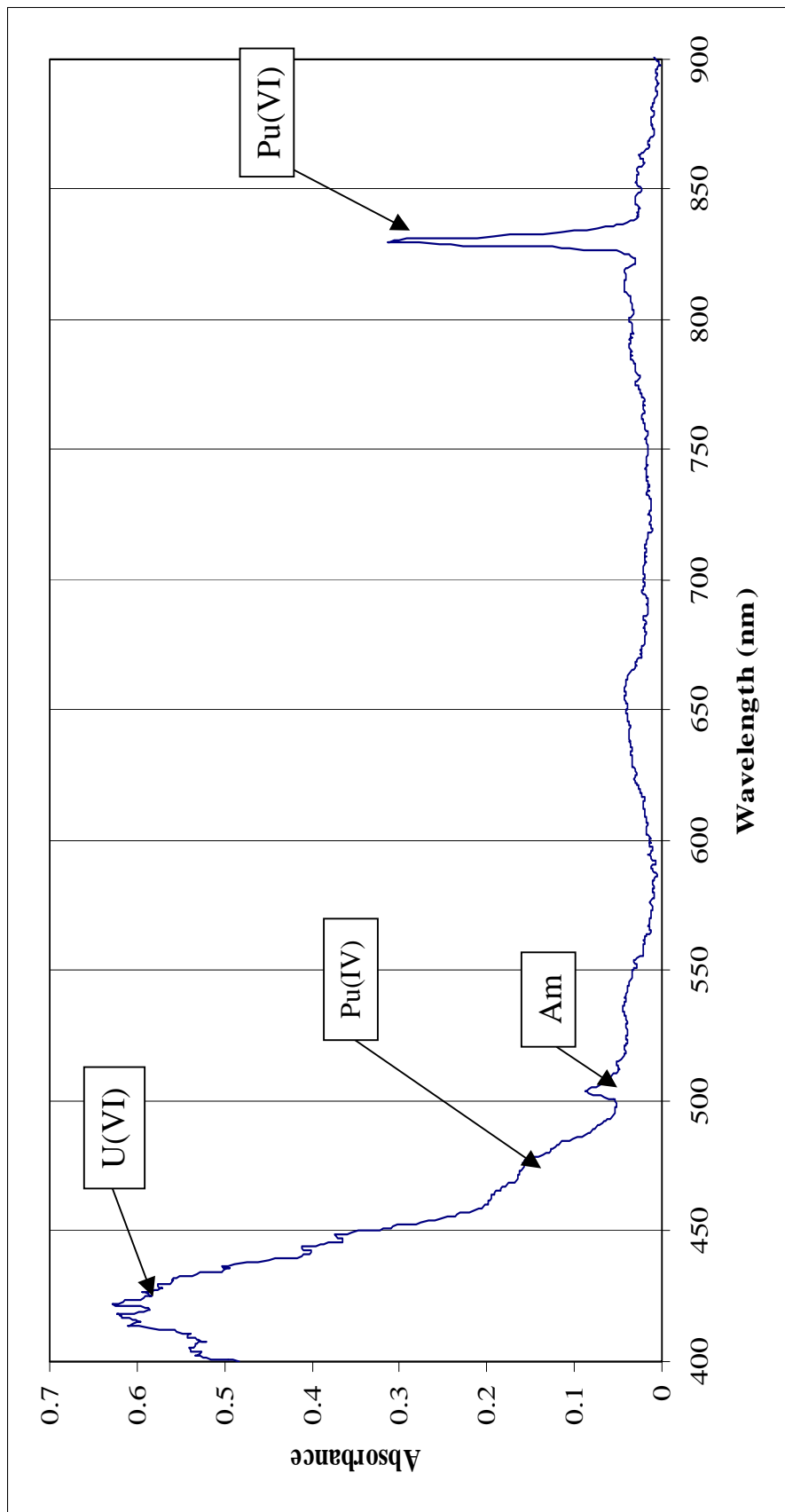


**Figure 2. UV-visible spectrum showing Pu(VI) peak at 830nm (evaporated MOX solution that was then treated to reduce Pu(VI) to Pu(IV) before using it for crystallisation tests)**

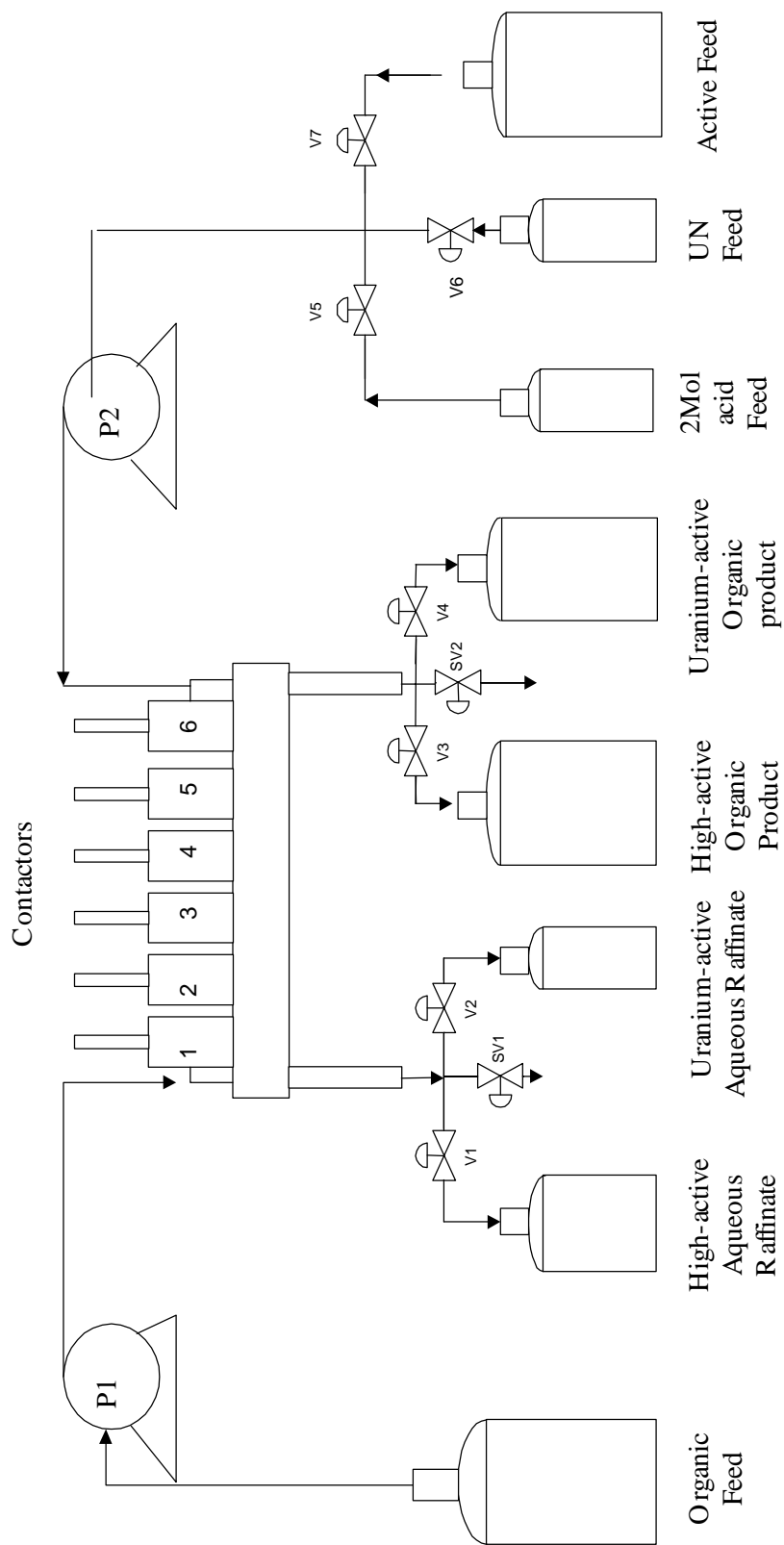


**Figure 3: Equipment arrangement for extraction**

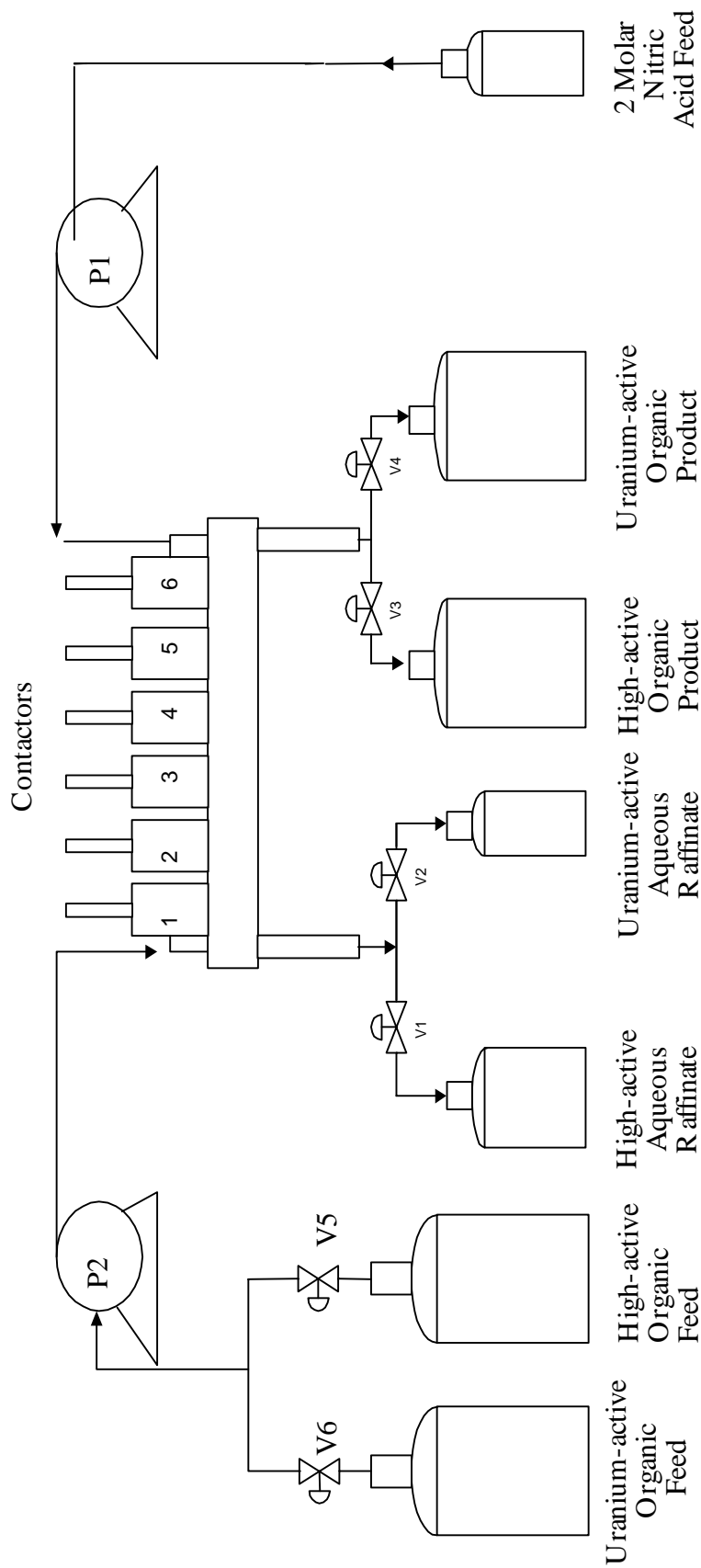


**Figure 4: Equipment arrangement for scrub**

# Appendix 2

## Photographs

---

### CONTENTS

Photograph 1. Rousselet/Robatel BXP012 rotor assembly from the side	app-7 (25)
Photograph 2. Close-up of Rousselet/Robatel BXP012 bowl, looking from above	app-8 (26)
Photograph 3. Complete Rousselet/Robatel BXP012 rotor and bowl assembly, looking from the side	app-9 (27)
Photograph 4. Close-up of Rousselet/Robatel BXP012 binding piece	app-10 (28)
Photograph 5. Complete assembly of Rousselet/Robatel BXP012 contactors, clamped with binding pieces to support rail	app-11 (29)
Photograph 6. Motor housing for Rousselet/Robatel BXP012 contactor, from below, showing recesses for central and peripheral pins on rotor assembly and coupling	
Photograph 7. Control panel for Rousselet/Robatel BXP012 contactors	app-12 (30)
Photograph 8. View of pump head for MOX feed with vernier setting gauge	app-13 (31)
Photograph 9. View of sampling tool in hot cell	app-14 (32)
Photograph 10. View of extraction arrangement.	app-15 (33)
Photograph 11. View of scrub arrangement	app-16 (34)



**Photograph 1. Rousselet/Robatel BXP012 rotor assembly from the side**



**Photograph 2. Close-up of Rousselet/Robatel BXP012 bowl, looking from above**



**Photograph 3. Complete Rousselet/Robatel BXP012 rotor and bowl assembly, looking from the side**

app-9(27)



**Photograph 4. Close-up of Rousselet/Robatel BXP012 binding piece (also showing detail of syringe sampling system, with clip released and needle lowered into sampling position on right-hand side)**

# Appendix 2

## Photographs

---

### CONTENTS

Photograph 1. Rousselet/Robatel BXP012 rotor assembly from the side	app-7 (25)
Photograph 2. Close-up of Rousselet/Robatel BXP012 bowl, looking from above	app-8 (26)
Photograph 3. Complete Rousselet/Robatel BXP012 rotor and bowl assembly, looking from the side	app-9 (27)
Photograph 4. Close-up of Rousselet/Robatel BXP012 binding piece	app-10 (28)
Photograph 5. Complete assembly of Rousselet/Robatel BXP012 contactors, clamped with binding pieces to support rail	app-11 (29)
Photograph 6. Motor housing for Rousselet/Robatel BXP012 contactor, from below, showing recesses for central and peripheral pins on rotor assembly and coupling	
Photograph 7. Control panel for Rousselet/Robatel BXP012 contactors	app-12 (30)
Photograph 8. View of pump head for MOX feed with vernier setting gauge	app-13 (31)
Photograph 9. View of sampling tool in hot cell	app-14 (32)
Photograph 10. View of extraction arrangement.	app-15 (33)
Photograph 11. View of scrub arrangement	app-16 (34)



**Photograph 1. Rousselet/Robatel BXP012 rotor assembly from the side**



**Photograph 2. Close-up of Rousselet/Robatel BXP012 bowl, looking from above**



**Photograph 3. Complete Rousselet/Robatel BXP012 rotor and bowl assembly, looking from the side**

app-9(27)



**Photograph 4. Close-up of Rousselet/Robatel BXP012 binding piece (also showing detail of syringe sampling system, with clip released and needle lowered into sampling position on right-hand side)**



**Photograph 5. Complete assembly of Rousselet/Robatel BXP012 contactors, clamped with binding pieces to support rail**



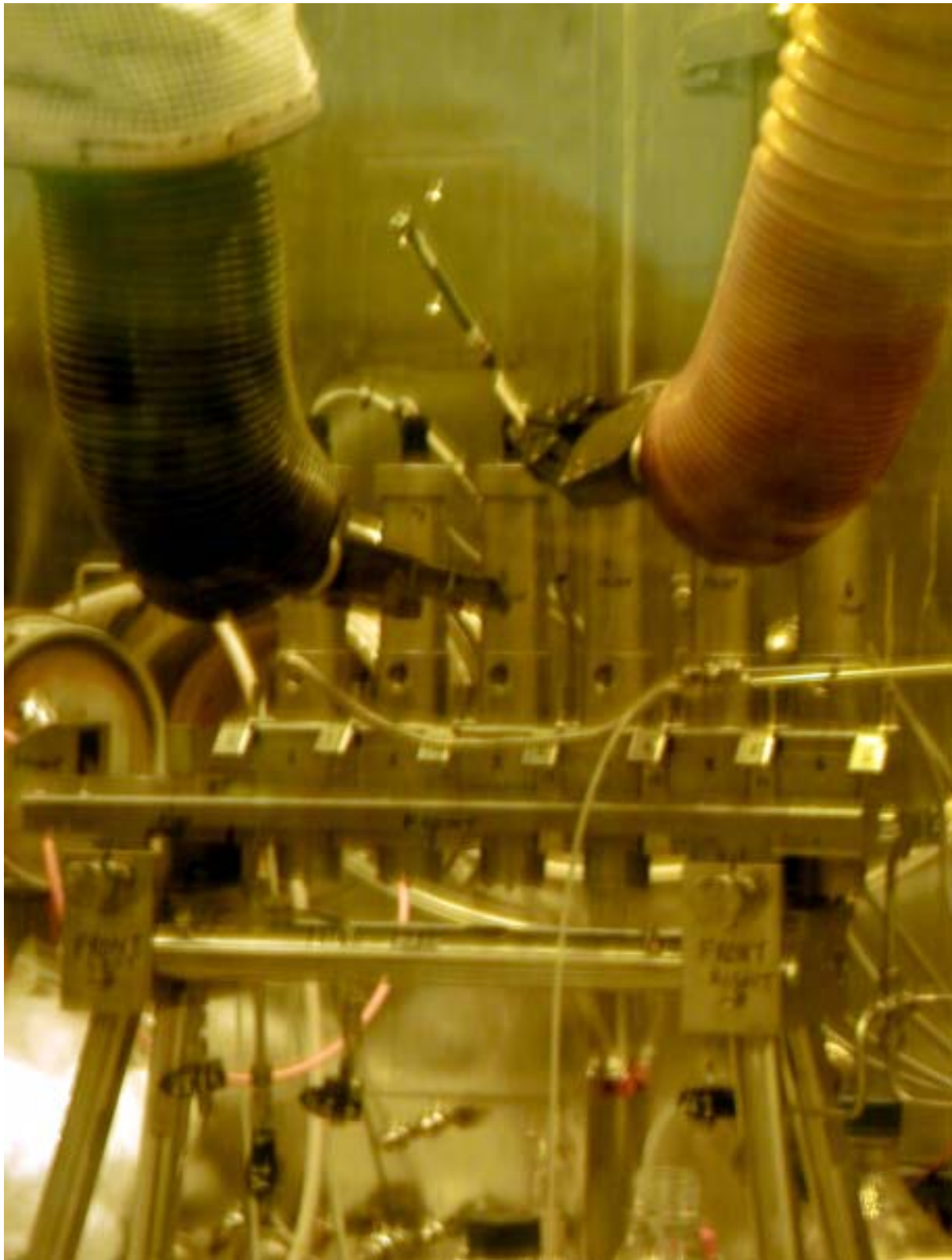
**Photograph 6. Motor housing for Rousselet/Robatel BXP012 contactor, from below, showing recesses for central and peripheral pins on rotor assembly and coupling**



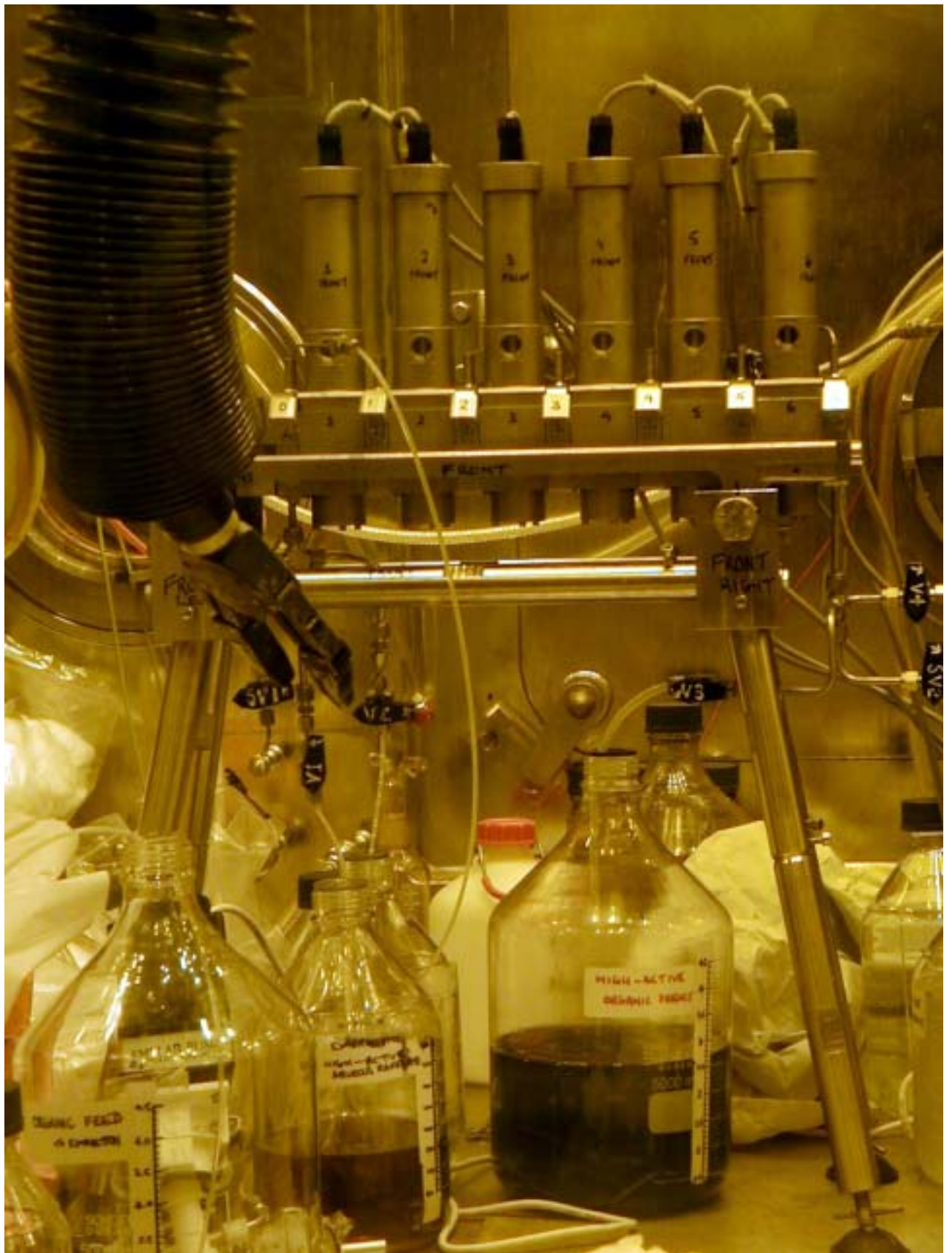
**Photograph 7. Control panel for Rousselet/Robatel BXP012 contactors**



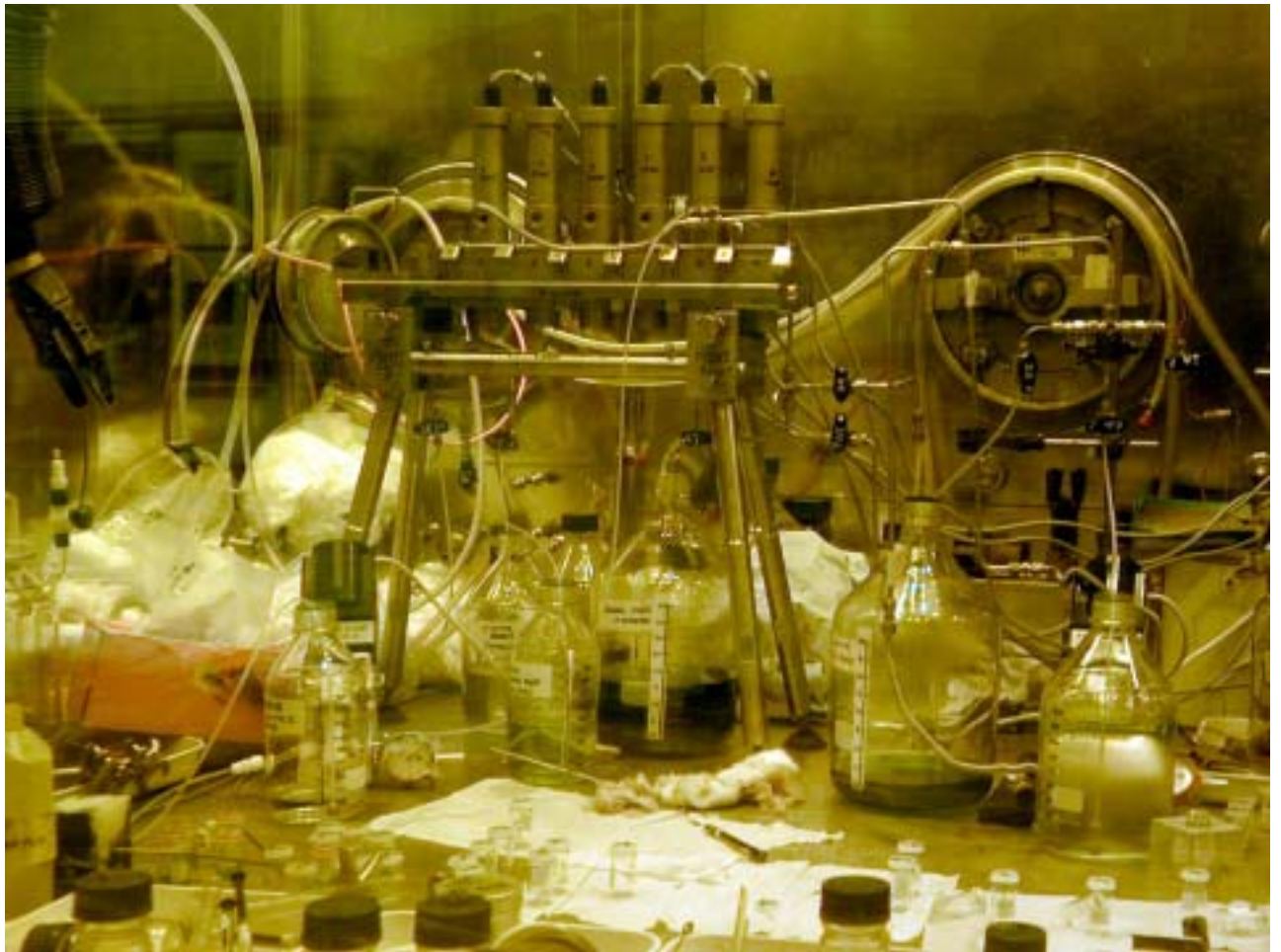
**Photograph 8. View of pump head for MOX feed with vernier setting gauge**



**Photograph 9. View of sampling tool in hot cell**  
(Right-hand manipulator is holding end of needle, with syringe barrel in upright position. Left-hand manipulator is used to pull the syringe plunger but is not in this position for clarity).



**Photograph 10. View of extraction arrangement, with high-active organic product on right-hand side and high-active raffinate on left-hand side**



**Photograph 11. View of scrub arrangement  
(high-active organic product and high-active raffinate under contactor support  
frame on right-hand and left-hand side respectively)**